

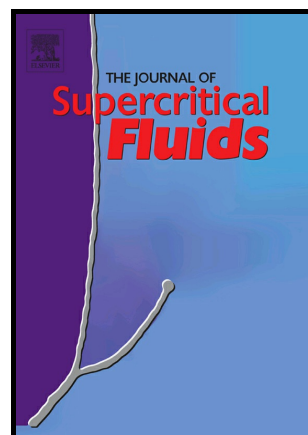
ULRR

Generation and physicochemical characterization of posaconazole cocrystals using gas antisolvent (GAS) and supercritical solvent (CSS) methods

Item Type	Article
Authors	Long, Barry;Verma, Vivek;Ryan, Kevin M.;Padrela, Luis
Citation	The Journal of Supercritical Fluids;170, 105134
Publisher	Elsevier
Download date	2026-03-06 23:26:58
Item License	https://creativecommons.org/licenses/by-nc-sa/1.0/
Link to Item	https://hdl.handle.net/10344/9611

Generation and Physicochemical Characterization of Posaconazole Cocrystals using Gas Antisolvent (GAS) and Supercritical Solvent (CSS) Methods

Barry Long, Vivek Verma, Kevin M Ryan, Luis Padrela



PII: S0896-8446(20)30385-5

DOI: <https://doi.org/10.1016/j.supflu.2020.105134>

Reference: SUPFLU105134

To appear in: *The Journal of Supercritical Fluids*

Received date: 29 May 2020

Revised date: 22 November 2020

Accepted date: 26 November 2020

Please cite this article as: Barry Long, Vivek Verma, Kevin M Ryan and Luis Padrela, Generation and Physicochemical Characterization of Posaconazole Cocrystals using Gas Antisolvent (GAS) and Supercritical Solvent (CSS) Methods, *The Journal of Supercritical Fluids*, (2020) doi:<https://doi.org/10.1016/j.supflu.2020.105134>

This is a PDF file of an article that has undergone enhancements after acceptance, such as the addition of a cover page and metadata, and formatting for readability, but it is not yet the definitive version of record. This version will undergo additional copyediting, typesetting and review before it is published in its final form, but we are providing this version to give early visibility of the article. Please note that, during the production process, errors may be discovered which could affect the content, and all legal disclaimers that apply to the journal pertain.

Generation and Physicochemical Characterization of Posaconazole Cocrystals using Gas Antisolvent (GAS) and Supercritical Solvent (CSS) Methods

Barry Long, Vivek Verma, Kevin M Ryan, Luis Padrela*

SSPC Research Centre, Department of Chemical Sciences, Bernal Institute, University of Limerick,
Limerick, Ireland

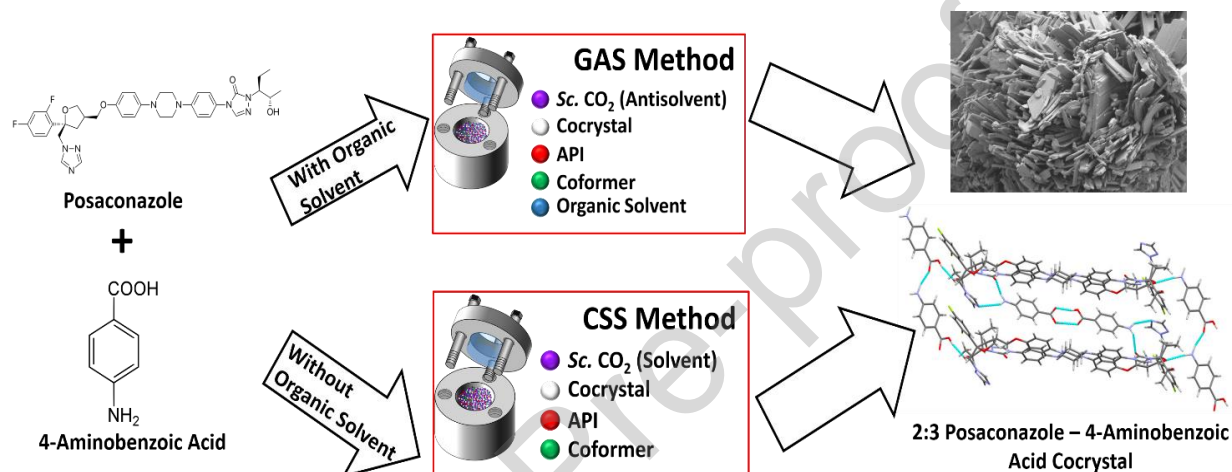
* Corresponding author: Luis.Padrela@ul.ie

Abstract

Posaconazole (PSZ) is a BCS (biopharmaceutical classification system) Class II anti-fungal drug used to treat infections in immunocompromised patients. The work presented herein describes the generation of cocrystals of PSZ with 4-aminobenzoic acid (4AMB) using supercritical CO₂ as an antisolvent in GAS (Gas Antisolvent) with acetonitrile, and as a solvent in CSS (Cocrystallization with Supercritical Solvent) methods. Cocrystals of PSZ-4AMB were obtained in a 2:3 stoichiometric ratio for the first time by GAS and CSS methods, with GAS producing higher-purity samples compared to CSS method. The work presented herein investigates the influence of critical processing variables using CO₂ solvent and antisolvent crystallization methods with respect to the formation of cocrystals of PSZ-4AMB. A Design of Experiments (DoE) approach was performed to assess the outcome of PSZ-4AMB formation, impacted by processing variables such as pressure, temperature, and stirring rate using GAS and CSS methods. The resulting cocrystalline phase was

identified using differential scanning calorimetry (DSC) and powder X-ray diffraction (PXRD). The particle morphologies and size distributions were determined using scanning electron microscopy and automated static imaging, respectively.

Graphical Abstract



Abbreviations

API, active pharmaceutical ingredient; PSZ, posaconazole; 4AMB, 4-aminobenzoic acid; GAS, gas antisolvent; CSS, cocrystallization with supercritical solvent; DSC, differential scanning calorimetry; PXRD, powder X-ray diffraction; FDA, food and drug administration; NCE, new chemical entity; MCC, molecular cocrystal; ICC, ionic cocrystal; BCS, biopharmaceutical classification system; SCF, supercritical fluid; scCO₂, supercritical CO₂; DoE, design of experiments; TGA, Thermogravimetric analysis; SEM, scanning electron microscopy; PSD, particle size distribution.

Keywords

Supercritical fluid, cocrystallization, particle engineering, CO₂, Posaconazole, Design of Experiment.

1.0 Introduction

Although pharmaceutical cocrystals have been studied for decades due to their ability to improve drug physicochemical and mechanical properties, they have recently attracted attention as they are also capable of extending the patent life of high-value drugs.[1, 2] In 2018, the Food and Drug Administration (FDA) clarified the classification of a cocrystal requiring these compounds to follow the same regulatory requirements as a polymorph of a drug compound, instead of applying the guidelines of a new chemical entity (NCE).[3] This ruling will encourage further research by both academia and the pharmaceutical industry into cocrystal systems as a result of this reduced testing required for FDA approval.[4]

The uncertainty surrounding cocrystal regulatory classification prior to the ruling in 2018 was emphasized by the controversy around the definition of a cocrystal. In 2012, the Indo-U.S. Science and Technology forum met and proposed a new cocrystal definition in an attempt to unify the controversy surrounding regulatory and academic definitions. This definition suggested that ‘cocrystals are solids that are crystalline single phase materials composed of two or more different molecular and/or ionic compounds generally in a stoichiometric ratio which are neither solvates nor simple salts’ .[5, 6] Cocrystals can be divided into two categories: molecular and ionic cocrystals. [7-10] Molecular cocrystals are crystalline solids that contain at least two compounds in a stoichiometric ratio while ionic cocrystals are multicomponent materials formed from a salt and a molecular or ionic compound.[1, 8, 9] Molecular cocrystals can be readily prepared by grinding or

slow evaporation and offer additional routes to generate cocrystals, particularly when a compound does not produce a salt, i.e. ionic cocrystal.[10, 11] Ionic cocrystals (ICC) offer stronger intermolecular bonding (coulombic forces and hydrogen bonds) than their molecular counterparts and the change in physicochemical properties is typically more dramatic, however, ICCs are, occasionally, not as thermodynamically stable as salts of the API.[10, 12, 13] Despite the vast amount of research into pharmaceutical cocrystals, there are currently only eight cocrystals approved by the FDA for use.[14] Of these eight cocrystals, four can be categorized as ionic and four as molecular.

Posaconazole (PSZ) is a BCS class II drug used in the treatment of antifungal infections in immunocompromised patients.[15] The aqueous solubility of PSZ is $< 1 \mu\text{g/mL}$ and as a result of this poor solubility, oral formulations containing PSZ currently in the market are in the form of a suspension and as an injectable.[16-18] The crystal structures of this active pharmaceutical ingredient (API) consist of a polymorph and a methanol solvate, which were only reported in 2019 by McQuiston et al. [19] Recently, Kuminek et al. have produced a 2:3 cocrystal of PSZ with 4-aminobenzoic acid (4AMB) by a reaction crystallization method and demonstrated a superior solubility compared to PSZ.[17] Supercritical fluid (SCF) technologies have existed for a long time but have only recently been investigated for their ability to generate pharmaceutical cocrystals.[20-27] Supercritical CO_2 (scCO_2) is the most commonly used SCF due to its low critical temperature (31.0 C) and pressure (7.4 MPa). In addition to this, scCO_2 is non-toxic, non-flammable and suitable for processing thermally labile pharmaceutical compounds. Supercritical CO_2 can be used as a solvent, antisolvent or as an additive for the generation of pharmaceutical compounds, including cocrystals. Active pharmaceutical model ingredients such as carbamazepine, curcumin, naproxen, resveratrol and ketoconazole have been used for the generation of cocrystals using supercritical fluid methods.[26, 28-34] Gas Antisolvent crystallization (GAS) is a method that was first proposed in

1989 which uses the antisolvent ability of scCO₂ for particle formation.[35, 36] In this method, CO₂ can be used in a gas, liquid or supercritical state where it is mixed with an organic solution containing an API until supersaturation is reached, which is concomitant with solution expansion and precipitation. In order for solvent expansion, and therefore precipitation, to occur, the CO₂ antisolvent should have little or no affinity for the API selected and the organic solvent should be readily miscible in CO₂ at the selected processing conditions. The phase behaviour between CO₂ and acetonitrile has been reported by Byun et al. who employed Peng-Robinson and SAFT models to describe the phase diagram between these two compounds at conditions similar to those employed in this study. In this study, Byun et al. describe that CO₂ and acetonitrile exhibit type 1 phase behaviour, characterized by an uninterrupted critical-mixture curve at three temperature points (35, 55 and 75 °C). At lower temperatures (35 °C), in order to achieve a 0.480 mole fraction of acetonitrile, 48.9 bar is required while at higher temperatures (75 °C) a higher pressure of 86.0 bar is required to achieve a similar (0.474) mole fraction.[29, 37-39] Since its discovery, the GAS method has become a popular approach for the generation of APIs and, more recently, pharmaceutical cocrystals as this method can remove time-consuming drying and filtration steps in addition to generating micron- and nano-sized particles.[22, 24-26, 28, 29, 38, 40, 41]

Another supercritical method, firstly reported as a method to generate indomethacin-saccharin cocrystals in 2009 by Padrela et al., utilizes scCO₂ as a solvent in a process named Cocrystallization with Supercritical Solvent (CSS).[42] The enhanced molecular mobility caused by the scCO₂ facilitates intermolecular interactions and, as a result, has promoted research to be conducted using this method for the development of pharmaceutical compounds such as cocrystals. [42-44] Recently Cuadra et al. reported the formation of cocrystals of the anticancer drug 5-fluorouracil using this methodology.[45] This method works, mechanistically, by forming a slurry between API and coformer, where some starting materials dissolve in scCO₂ and react to generate a

cocrystal. This process is repeated until the contents have fully reacted, provided sufficient reaction time and suitable operating conditions such as temperature and pressure (which influence CO₂ density and consequently the amount of API and coformer dissolved in scCO₂) and stirring rate (which influences homogeneity in the cocrystallization medium, being determinant for the enhancement of the intermolecular interactions between the pure components) [44] are achieved, and the cocrystal is in the thermodynamically favored phase. The primary advantage of the CSS method, compared to the GAS method, involves the significant reduction or elimination of organic solvent, thereby removing filtration and secondary drying steps from the process. However, CSS is constrained by the requirement for the starting materials used to have a minimum level of solubility in scCO₂, so that cocrystallization may occur. To the best of our knowledge the solubility of PSZ in scCO₂ is not available, however, the solubility of the coformer 4AMB in scCO₂ has been investigated by Tian et al.[46] The solubility of 4AMB was shown to have a relatively low value compared to other compounds that have been previously processed by the CSS method.[22]

In this work both GAS (uses scCO₂ as an antisolvent) and CSS (uses scCO₂ as a solvent) methods were used to investigate if different processing parameters (pressure, temperature and stirring rate) which are known to impact the solid state of APIs can affect the PSZ-4AMB cocrystallization. The results from both methods are compared using a range of characterization techniques such as powder X-ray diffraction, electron microscopy, thermal analysis and particle size distribution analysis.

2.0 Experimental Section

2.1 Materials

Posaconazole (PSZ) was purchased from Kemprotec Ltd. at 98% purity and used without any modifications. Acetonitrile, methanol and 4-Aminobenzoic acid (4AMB) were purchased from

Sigma Aldrich and used without further purification (purity was >99.9%). Both PSZ and 4AMB were characterized by PXRD (powder X-ray diffraction) to confirm its raw crystalline form. Carbon dioxide (99.98%) was supplied by BOC (Ireland). The molecular structures of PSZ and 4AMB and the desired cocrystal, PSZ-4AMB are presented in Fig. 1. The structures of PSZ, 4AMB and PSZ-4AMB were drawn using ChemDraw software, version 11.

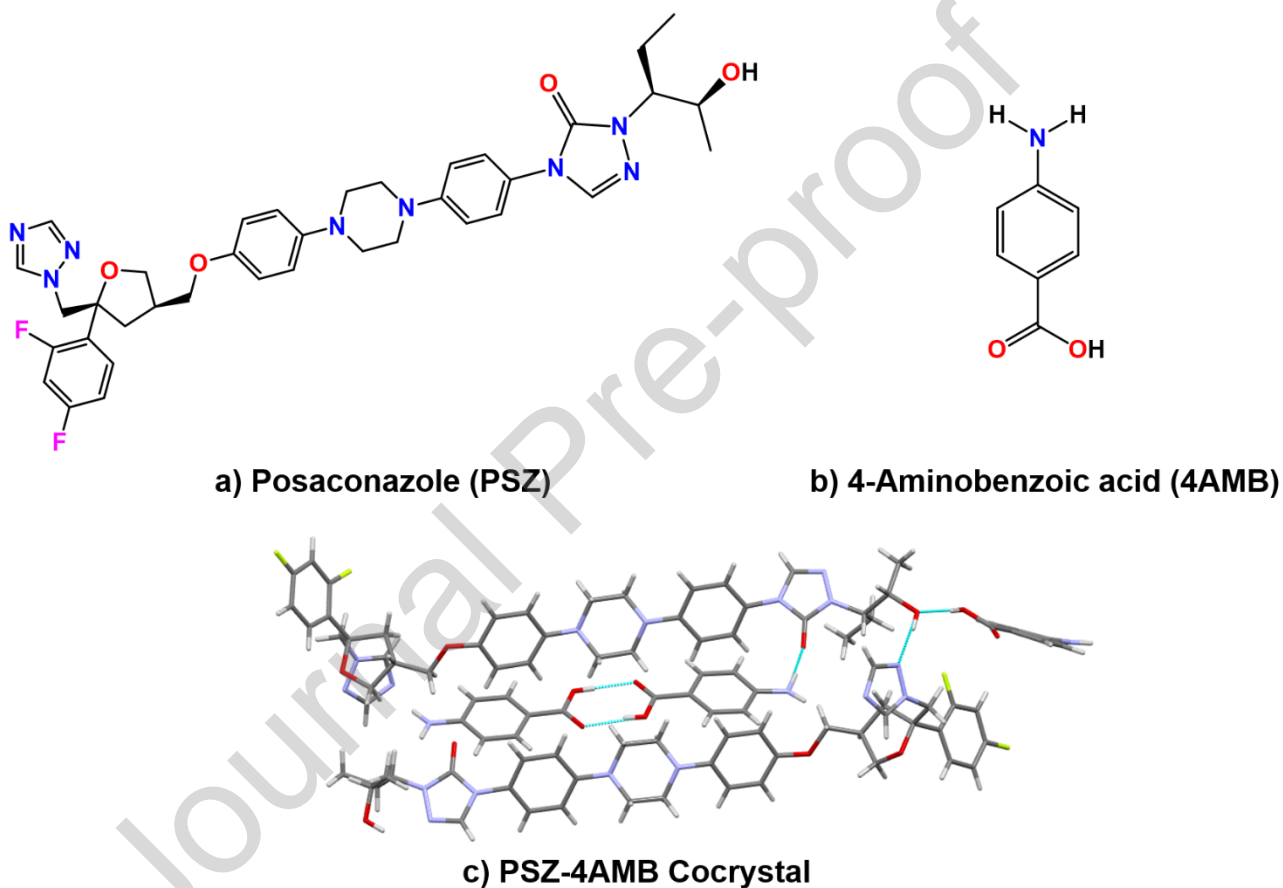


Figure 1. Molecular structures of a) posaconazole, b) 4-aminobenzoic acid and (c) PSZ-4AMB cocrystal.

2.2 Gas Antisolvent (GAS) and Cocrystallization with Supercritical Solvent (CSS) setup

Figure 2 presents a schematic diagram of a custom-designed Gas Antisolvent (GAS) and Cocrystallization with Supercritical Solvent (CSS) setup, describing the contrasting mechanisms between both methods. In the GAS method, the API and coformer are first dissolved in an organic

solvent, whereas in the CSS method no organic solvent is used.

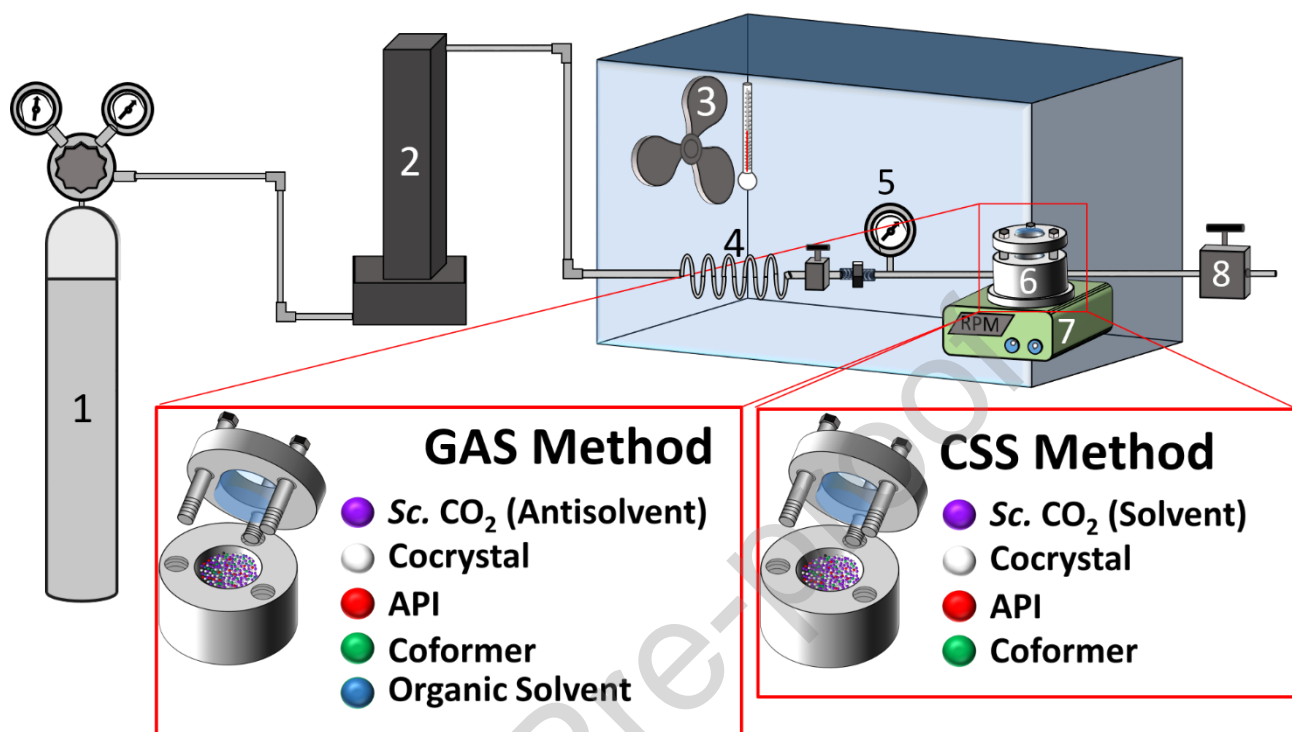


Figure 2. Schematic diagram of the Gas Antisolvent (GAS) and CocrySTALLIZATION by Supercritical Solvent (CSS) apparatus. 1, CO₂ cylinder; 2, liquid compressor; 3, temperature-controlled air chamber; 4, stainless steel storage coil; 5, pressure transducer; 6, high-pressure vessel; 7, magnetic stirrer plate; 8, exit valve.

The high-pressure setup, used for both GAS and CSS methods, presented in Fig. 2 consists of a 15 cm³ stainless steel storage coil and a 10 cm³ (8.83 cm³ working volume) stainless steel high-pressure reaction vessel (where precipitation/crystallization occurs) with monitored temperature and pressure using a T-type thermocouple and a pressure transducer (Omega model PX603), respectively. The temperature of these vessels was maintained using a temperature-controlled air chamber. This ensured that the CO₂ remained in a supercritical state throughout the experiments and ongoing reactions were completed at a constant temperature. A borosilicate window was fitted on the top of the high-pressure vessel for visualization purposes during the experiments. A Teledyne ISCO 260D pump was used to compress the CO₂ before discharging it into the storage coil where it was allowed

to remain for a short period of time (~10 minutes) until it reached the desired temperature. For GAS experiments, 10 mg of PSZ and 3 mg of 4AMB were weighed out and dissolved in 1 ml of acetonitrile. The amount of PSZ and 4AMB used for the GAS method was based on the maximum solubility (10.4 mg/ml) of PSZ in acetonitrile at ambient conditions so that a saturated PSZ solution could be processed.[47] This value was significantly lower than the solubility of 4AMB in acetonitrile at the same conditions (90.6 mg/ml) and was the limiting factor for the low combined quantity of API and coformer used in the GAS method.[48] Additionally, the low working volume of the high-pressure vessel (8.83 cm³) limits the amount of solution (1 ml) that can be placed inside. If greater volumes are required, the pressure of the scCO₂ must be increased to ensure that supersaturation conditions are satisfied. The maximum pressure that the borosilicate window can withstand is 20.0 MPa and this is the limiting factor for the low volume of solution added to the vessel. The solutions were subjected to ultrasonic treatment for a period of approximately 5 minutes to ensure all starting material had dissolved. Acetonitrile was selected as it was the solvent selected to produce the 2:3 cocrystal of PSZ-4AMB as other solvents such as methanol, which is frequently used in scCO₂ antisolvent processing, resulted in the formation of a PSZ-Methanol solvate. [17, 19] An experiment was conducted using methanol to investigate if this solvate would form through supercritical processing. PXRD results confirming the formation of PSZ-methanol solvate using the GAS method is reported in the supplementary material, Fig. SM2. An acetonitrile solution containing PSZ and 4AMB dissolved was placed inside the 10 cm³ reaction vessel and sealed. Magnetic stirring (stirrer bar: 6 mm x Ø 3 mm) was switched on and scCO₂ was then allowed to flow into the high-pressure vessel at a rate of 46 g/min until the desired pressure, reported in tables 1 and 2, was reached. After approximately 5 minutes, magnetic stirring was turned off and the exit valve (number 8 in Fig. 2) was opened to continuously flush scCO₂ through the high-pressure vessel, thereby removing the expanded acetonitrile from the high-pressure reaction vessel (number 6

in Fig. 2). Once magnetic stirring had been switched off, the suspended particles settled down to the bottom of the vessel during the flushing step. The scCO₂ was passed through the reaction vessel over a 1-hour time frame at a flow-rate of 5 g/min (dependent on the pressure and temperature used). For CSS experiments, as no organic solvent was required, 50 mg of PSZ and 15 mg of 4AMB were weighed and directly placed in the reaction vessel and sealed. The addition of scCO₂ and magnetic stirring remained the same as described in the GAS method. These materials remained suspended inside the high-pressure vessel for approx. 1 hour (until magnetic stirring was switched off) to maintain identical reaction times experienced by the GAS method. Once completed, magnetic stirring was turned off and the exit valve (number 8 in Fig. 1) was opened to immediately depressurize the reaction vessel. Once depressurization of the vessel had concluded for GAS and CSS methods, the resulting materials were collected and stored in a desiccator prior to their characterization to minimize the occurrence of solid state transformations. Tables 1 and 2 present the operating conditions used in GAS and CSS experiments, respectively. The dimensions of the high-pressure vessel, borosilicate glass window and stirrer bar are provided in Fig. SM1 in the supplementary material.

2.3 Design of Experiments (DoE)

A study using a 3-factor 2-level full factorial Design of Experiments (DoE) was performed to investigate the influence of different processing parameters on the formation of PSZ-4AMB cocrystals. Three factors on which the DoE was based are pressure, temperature and stirring rate. Maximum and minimum values were selected and will be discussed in greater detail below. Table 1 describes the operating parameters and values selected for all DoE points using the GAS method. Additionally, this table describes if the final form obtained was the desired PSZ-4AMB cocrystal or undesired API, coformer or mixture. Each of the DoE experiments were performed in duplicate to ensure repeatability.

Table 1. Experimental Conditions Used in Gas Antisolvent (GAS) Experiments for Posaconazole-4Aminobenzoic Acid Formation using a Design of Experiments (DoE) Approach^a

Cocrystal System	DoE Point	Pressure (MPa)	Temperature (° C)	Stirring Rate (RPM)	Solid Form Obtained
PSZ-4AMB	1	10.0	35	100	Cocrystal + Minor PSZ Impurities
	2	20.0	35	100	Cocrystal + Minor PSZ Impurities
	3	10.0	65	100	Cocrystal + Minor PSZ Impurities
	4	20.0	65	100	PSZ
	5	10.0	35	1000	Cocrystal + Minor PSZ Impurities
	6	20.0	35	1000	Cocrystal + Minor PSZ Impurities
	7	10.0	65	1000	Cocrystal + Minor PSZ Impurities
	8	20.0	65	1000	Cocrystal + Minor PSZ Impurities

^a For all DoE points; a 2:3 stoichiometric ratio was used between API (PSZ) and coformer (4AMB); concentration of initial solution was 10 mg of PSZ and 3 mg of 4AMB dissolved in 1 ml of acetonitrile and reaction vessel was flushed for approximately one hour with scCO₂ at a rate of 5 g/min.

Table 2 describes the operating parameters, values and solid state forms obtained for all DoE points (9-16) using the CSS method.

Table 2. Experimental Conditions Used in Cocrystallization by Supercritical Solvent (CSS) Experiments for Posaconazole-4Aminobenzoic Acid Formation using a Design of Experiments (DoE) Approach^b

Cocrystal System	DoE Point	Pressure (MPa)	Temperature (° C)	Stirring Rate (RPM)	Solid Form Obtained
PSZ-4AMB	9	10.0	35	100	PSZ + 4AMB + Minor Cocrystal
	10	20.0	35	100	Cocrystal + PSZ + 4AMB
	11	10.0	65	100	Cocrystal + PSZ
	12	20.0	65	100	Cocrystal + PSZ
	13	10.0	35	1000	Cocrystal + PSZ +4AMB
	14	20.0	35	1000	Cocrystal + PSZ
	15	10.0	65	1000	Cocrystal + PSZ + 4AMB
	16	20.0	65	1000	Cocrystal + PSZ

^b For all DoE points; a 2:3 stoichiometric ratio was used between API (PSZ) and coformer (4AMB); 50 mg of PSZ and 15 mg of 4AMB were directly placed in the vessel, immersed in scCO₂ and stirred for a period of one hour; upon completion, the vessel was immediately depressurized and sample collected.

2.4 Solid-state characterization

2.4.1 Powder X-ray Diffraction (PXRD)

Powder X-ray diffraction (PXRD) in reflection mode was performed using an Empyrean diffractometer (PANalytical, Phillips) with Cu K α radiation ($\lambda = 1.5406 \text{ \AA}$) at room temperature. Samples were lightly ground and pressed on a zero-background plate prior to analysis. Data was recorded at a tube voltage of 40 kV and a tube current of 40 mA, with a step size of 0.02° (2θ) and a scan speed of 0.102° ($2\theta \cdot \text{s}^{-1}$) in the angular range of 5° to 30° (2θ) with 4 RPM.

2.4.2 Scanning Electron Microscopy (SEM)

Scanning Electron Microscopy (SEM) analysis was performed on a Hitachi SU-70 system operating at 3 kV. Samples were mounted onto aluminum stubs with double-sided carbon tape. The stubs were placed inside a gold sputter coater (Emitech K550X) and coated with a plasma current of 20 mA for two minutes.

2.4.3 Particle Size Analysis

Particle size analysis of PSZ-4AMB samples were determined using a Malvern Morphologi G3SE particle characterization system (Malvern Instruments, Malvern, UK). Samples were dry dispersed using the systems automated sample dispersion unit (5541 mm² area) onto a glass plate (180 \times 110 mm) with an injection pressure of 0.4 MPa, an injection time of 10 ms and a setting time of 60 s. A range of particle size from 0.5 μm to 40 μm were quantified using 50X (Nikon TU plan

ELWD) magnification optics selection. The system works by imaging every particle and as such reports a number-based particle size distribution.

2.4.4 Thermal Analysis

Thermogravimetric analysis (TGA) was performed using a Perkin Elmer TGA 4000 at a constant heating rate of 10 °C/min from 25 to 340 °C under a 50 ml/min flux of nitrogen on a sample to determine a suitable range for further analysis. This data is presented in the supplementary material, Fig. SM3. Differential scanning calorimetry (DSC) was carried out using sealed aluminum pans on a TA Instruments Netzsch Polyma 214 differential scanning calorimeter at a range of 50 to 275 °C. Temperature calibrations were made using indium as the standard. An empty pan, sealed in the same way as the sample, was used as a reference. All the thermogram data was collected at a heating/cooling rate of 10 °C/min under a nitrogen purge at a rate of 50 ml/min.

2.4.5 Fourier Transform Infrared

The FTIR spectrum of the samples was measured at an ambient temperature using a Perkin-Elmer Spectrum 100 FTIR spectrometer. The spectrum was collected at wavelengths of 4000–650 cm^{-1} using an attenuated total reflection accessory with a ZnSe crystal. Samples were uniformly spread on the crystal with a pushing arm and 50 scans were collected for each sample at a resolution of 4.00 cm^{-1} . This data is illustrated in the supplementary material, Figs. SM4 and SM5.

3.0 Results and Discussion

3.1 Cocrystallization and characterization of PSZ-4AMB by Gas Antisolvent (GAS) method

A Design of Experiments (DoE) approach was used and three processing parameters (e.g. pressure, temperature and stirring rate) were selected to investigate their impact on PSZ-4AMB cocrystal

formation. Several considerations were taken when deciding the maximum and minimum parameter values which are discussed further below. As reported by Chang et al., the density of scCO₂ is directly related to the pressure used, and a higher pressure (denser scCO₂) increases the proportion of organic solvent dissolved in scCO₂.^[49] Prior to conducting this DoE, preliminary experiments were performed at the least dense scCO₂ values (low pressure, high temperature and low stirring rate) to ensure that precipitation at these points, the least likely to induce crystallization, would occur. The minimum pressure value selected was 10.0 MPa to ensure that CO₂ would remain in a supercritical state while 20.0 MPa was selected as the maximum pressure value due to the pressure rating of the equipment. The minimum temperature setting employed was 35 °C based on the critical temperature of scCO₂ of 31.0 °C, while the maximum temperature setting was selected based on the maximum value permitted for the equipment. Finally, stirring was selected as a process parameter in the DoE as it is known to have an influence on crystallization properties such as particle size but has not been investigated for its impact on cocrystal formation using supercritical methods.^[31] From the initial experiments conducted before examining DoE points, it was discovered that while precipitation did eventually occur, it was not immediate and took approximately 2 minutes for it to be observed after the desired pressure value was achieved. For this reason, during GAS processing the contents of the high-pressure vessel were subjected to stirring for a period of 5 minutes to ensure precipitation had taken place.

The solid-state form of the GAS samples was determined using Powder X-Ray Diffraction (PXRD) by comparing the patterns from each sample to the reported cocrystal pattern by Kuminek et al., and to raw PSZ and 4AMB.^[17] This data is presented in Fig. 3.

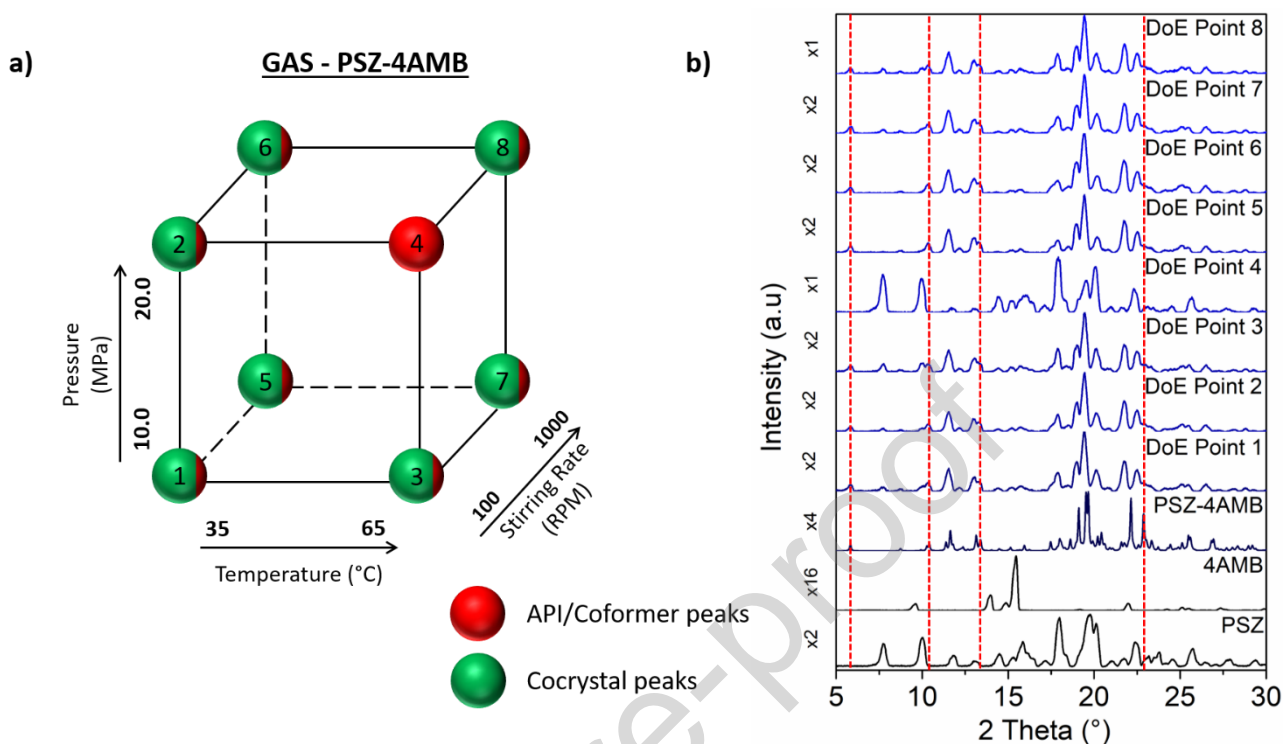


Figure 3. a) Design of Experiments (DoE) schematic to investigate the impact of pressure, temperature and stirring rate as the process variables on PSZ-4AMB formation using the Gas Antisolvent (GAS) method. b) Powder X-ray diffraction patterns of raw PSZ, raw 4AMB and theoretical PSZ-4AMB cocrystal from the Cambridge Structural Database (CSD)[17] and DoE samples processed by the GAS method. Experimental conditions as described in Table 1 (DoE Points 1-8). Red dotted lines, highlighting characteristic cocrystal peaks, are included at 5.5 °, 10.5 °, 13 ° and 22.8 ° 2 Theta.

For the samples produced by the GAS method (DoE Points 1-8), a large proportion of these (7 out of 8) resulted in the formation of the PSZ-4AMB cocrystal, identified by four characteristic peaks described in Fig. 3b. The samples that appeared to correspond to high-purity PSZ-4AMB matched most of these characteristic peaks with the exception of the peak at 22.8 ° 2 Theta. A shoulder peak can be observed at this 2 Theta value, however, it is not clear that it is related to this cocrystal peak and lacks the intensity observed by the other PSZ-4AMB characteristic peaks. From the 7 points that produced the PSZ-4AMB cocrystal, two peaks at 8.1° and 27.6° 2 Theta, which correspond to PSZ, can still be identified in five of these samples (DoE points 1,2,3,7 and 8); while DoE points 5

and 6 only possess one of these peaks at 27.6°. However, this impurity is present in very low amounts and these samples can still be categorized as high-purity PSZ-4AMB cocrystals. Due to the minor amounts of PSZ peaks detected and absence of 4AMB peaks in all samples, excluding DoE point 4, this result may suggest that some of the coformer (4AMB) was removed during the flushing step. Additionally, most of the 4AMB is consumed during the cocrystallization step and the remaining quantity of unreacted 4AMB may have been in such small quantities that it could not be detected by PXRD. This is supported by a significantly increased solubility of 4AMB (relative to PSZ) in acetonitrile.[47, 48] Only one GAS sample (DoE point 4) resulted in PXRD-pure PSZ. The conditions for this point were 20.0 MPa, 65 °C and 100 RPM. One possible explanation for the low-purity cocrystal sample is that the onset of antisolvent supersaturation is slower at 100 RPM than at 1000 RPM, taking it longer for the CO₂ to mix with the PSZ-4AMB acetonitrile solution and supersaturate it. This gradual supersaturation may favor the precipitation of PSZ first rather than the cocrystal mixture, as high-purity PSZ-4AMB is detected for the same conditions at a high stirring rate (1000 RPM). This assumption would require further work into investigating the solubility of both components (PSZ and 4AMB) in scCO₂ to verify this prediction.

Figure 4 presents SEM micrographs and PSD analysis of the different samples from the DoE points 1-8 (Fig. 3a) produced by the GAS method. To date, there are no SEM micrographs of this cocrystal available in the literature, therefore the crystal habit of this cocrystal is unknown and hence, cannot be compared.

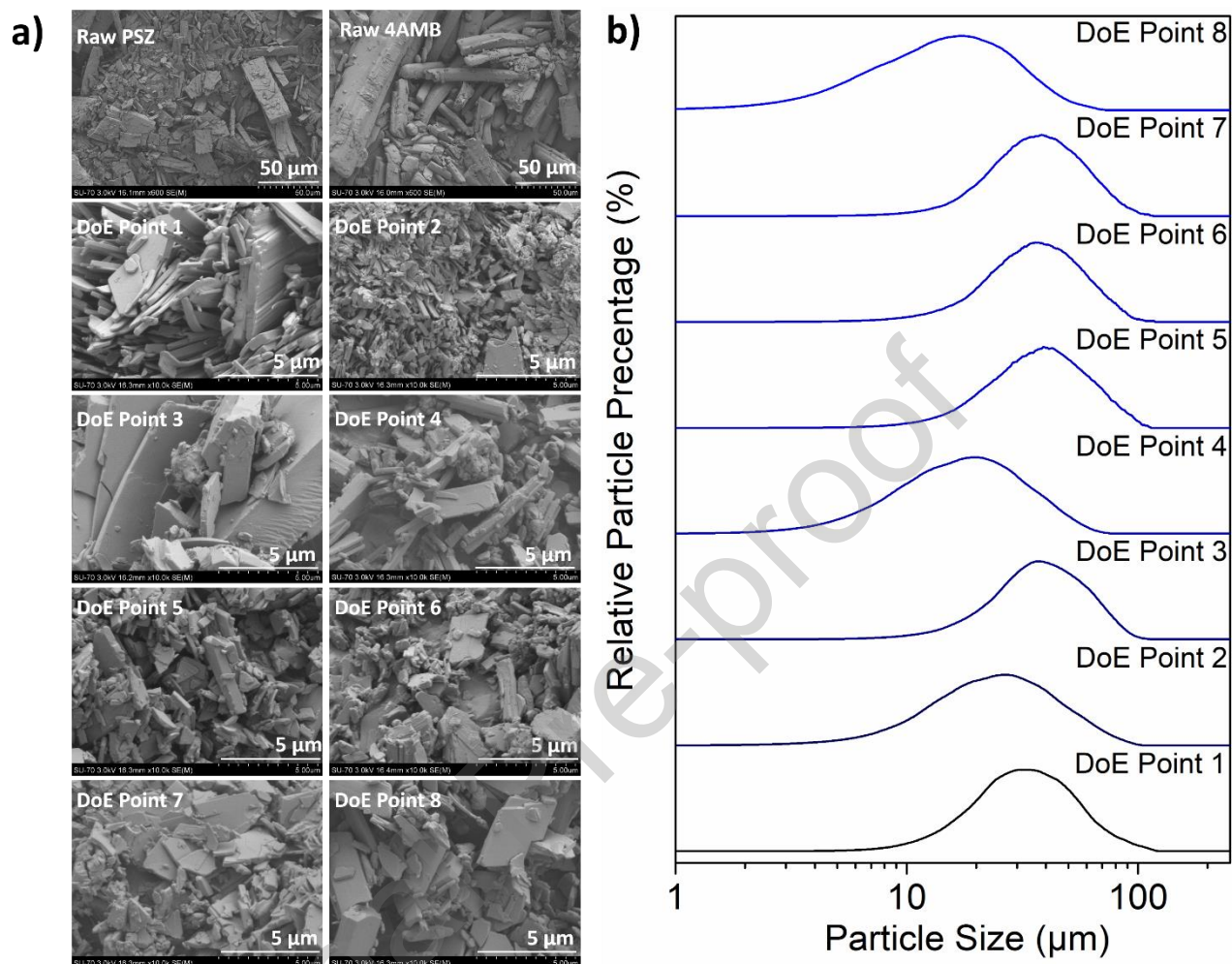


Figure 4. a) Scanning electron microscopy micrographs of raw PSZ, 4AMB and PSZ-4AMB samples (DoE points 1-8) and b) particle size distribution (PSD) of PSZ-4AMB samples (DoE Points 1-8) produced by the Gas Antisolvent (GAS) method.

From the SEM micrographs in Fig. 4a, the crystal habit of the PSZ-4AMB cocrystals appear to be plate-like. This crystal habit of PSZ-4AMB is similar to raw PSZ, while raw 4AMB has a rod-like habit. Distinguishing between PSZ and PSZ-4AMB cocrystals using SEM techniques is a challenging task due to similarities in the crystal habit of both compounds. The particles presented in Fig. 4a for DoE point 4, which were shown to be PXRD-pure PSZ, appear to be visually similar to the other particles produced by this method (DoE points 1, 2, 3, 5, 6, 7, 8), emphasizing the similarity between API and cocrystal habits. The only noticeable difference in these micrographs is

for DoE point 3 which appears to show slightly larger particles than other samples, however this is not observed in the PSD for this sample in Fig. 4b. The SEM analysis in this Fig. 4b is intended to identify the crystal habit of PSZ-4AMB and does not analyze the same number of particles as PSD analysis. Based on the SEM micrographs, Fig. 4a suggests that particles within the samples produced from DoE points 2 and 5 appear to be smaller than those produced from other samples (DoE points 1, 3, 4, 6-8), however, these micrographs may not be representative of the entire sample and will only be used to determine crystal habit in this study. The particle size analysis for GAS samples are provided in Fig. 4b and demonstrate an average particle diameter range of 20 – 43 μm . Two samples (DoE points 4 and 8) show a lower but wider than average PSD (D_{50} of 21 and 20 μm , respectively) and both of these points share high temperature (65 $^{\circ}\text{C}$) and high pressure (20.0 MPa) values. Although the sample produced at DoE point 4 does not show any evidence of the PSZ-4AMB cocrystal, shown in Fig. 3, the conditions used are still investigated with respect to particle size, especially since this DoE point provides below average particle sizes. Surprisingly, stirring rate does not appear to significantly influence the PSD at either of these points. The remaining samples (DoE points 1, 2, 3, 5, 6 and 7) demonstrate minimal deviation from the median PSD (36 μm) and suggest that samples produced at these combinations of processing conditions do not influence the particle size during GAS processing.

Figure 5 presents the DSC data for PSZ-4AMB samples (DoE Points 1-8) produced by the GAS method.

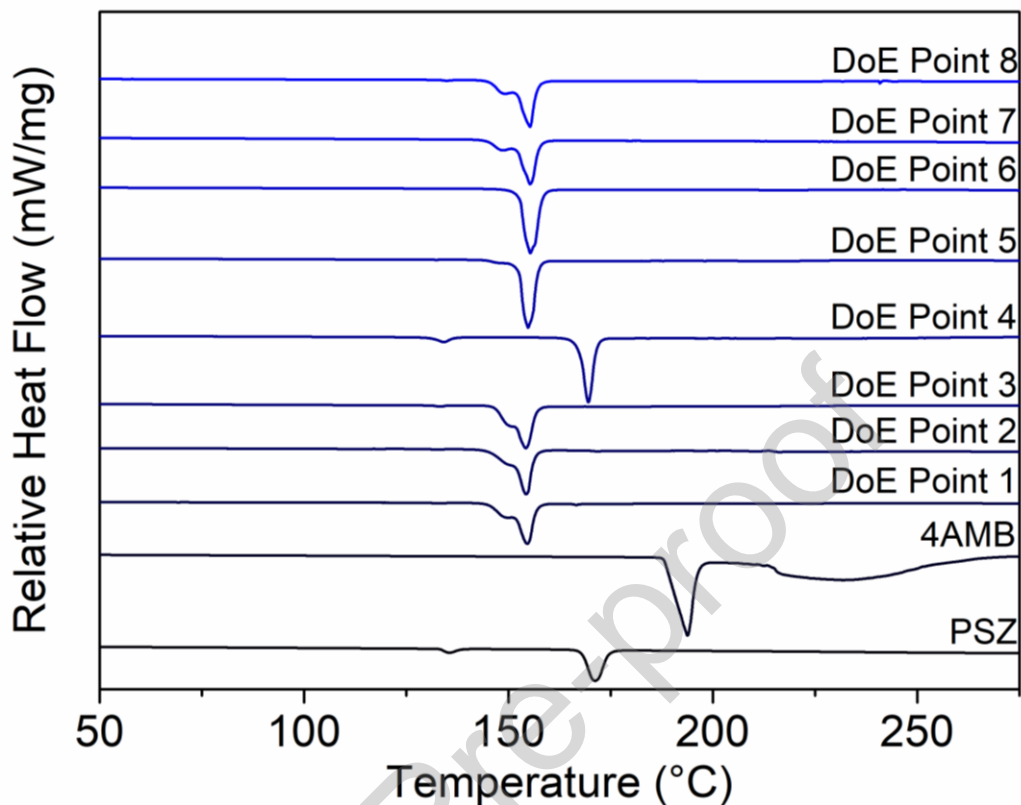


Figure 5. Differential scanning calorimetry (DSC) thermograms of raw PSZ, raw 4AMB and samples for DoE Points 1-8 produced by the GAS (Gas Antisolvent) method.

The thermal behaviour of the PSZ-4AMB cocrystal, reported by Kuminek et al., presents a single endothermic event at 154.1 °C.[17] This differs from the thermal behaviour of PSZ which demonstrates a nematic-like phase transition at 134 °C followed by a melting point at 168.2 °C, in addition to the thermal behaviour of 4AMB which melts at 188.3 °C. The results of the DSC analysis in Fig. 5 shows a melting point at 154 °C for most samples (DoE points 1, 2, 3, 5, 6, 7 and 8) which showed evidence of cocrystal formation. The GAS sample which demonstrated to be PXRD-pure PSZ (DoE Point 4) presented thermal behaviour corresponding to raw PSZ. However, five out of seven DoE points (DoE points 1,2,3,7 and 8) possess a shoulder peak at 148 °C which may correspond to small amount of impurities from PSZ, which was observed from the PXRD

analysis in Fig. 3. Two GAS samples (DoE Point 5 and 6) demonstrate a single melting point at 154 °C in Fig. 5, indicating a sample of greater purity. This result is supported by PXRD analysis which report the absence of the PSZ impurity peak at 8.1° (2θ) for these two samples in Fig. 3.

3.2 CocrySTALLIZATION and characterization of PSZ-4AMB by CocrySTALLIZATION by Supercritical Solvent (CSS) method

In order to compare the effectiveness of the GAS and CSS methods for the formation of PSZ-4AMB cocrySTALS, the DoE processing parameters for the CSS method (see Table 2) were kept the same as reported in Table 1. The duration that the starting materials (API and coformer) were immersed in scCO₂ was approximately 1 hour. This duration was selected ensuring that there was consistency between the flushing time employed for the GAS method and immersion time for the CSS method with all other parameters remaining unchanged. No preliminary experiments were completed using this method, unlike in the GAS method, as no visual indicators, such as precipitation, could be observed to suggest that a reaction has occurred.

Figure 6 presents the PXRD data of samples produced by the CSS method compared to the reported theoretical pattern for PSZ-4AMB, raw PSZ and 4AMB.

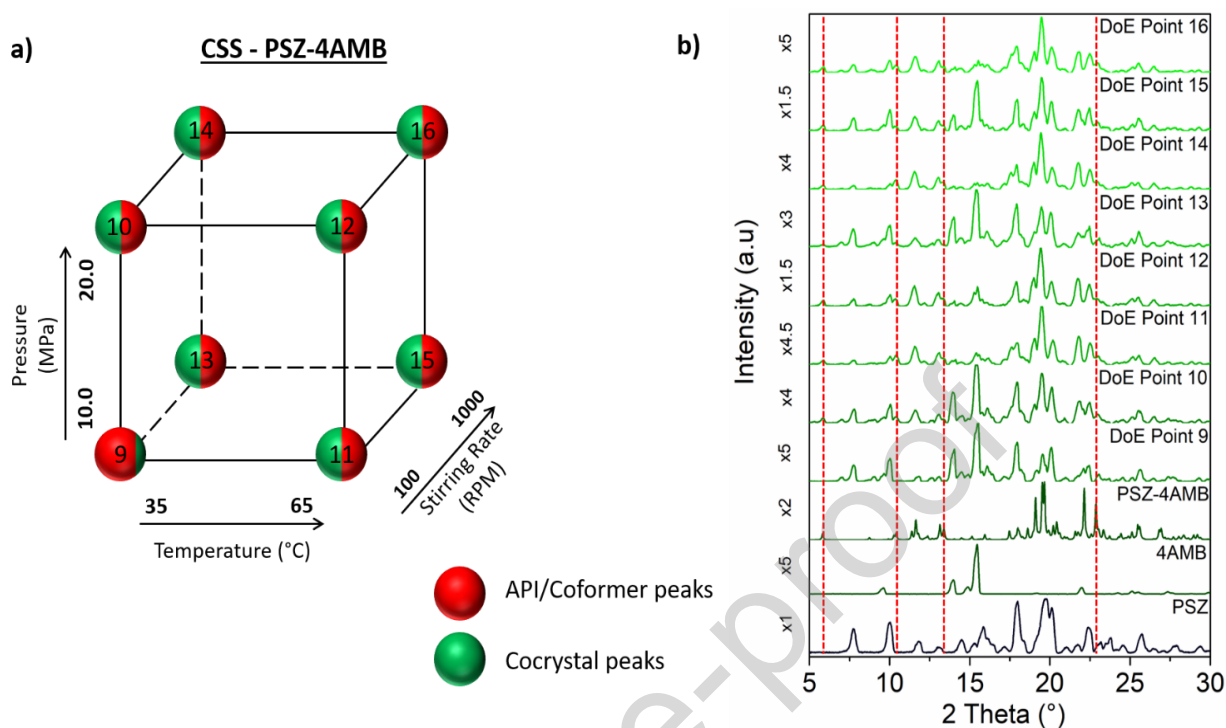


Figure 6. a) Design of Experiments (DoE) schematic to investigate the impact of pressure, temperature and stirring rate as the process variables on PSZ-4AMB formation using the Cocrystallization with Supercritical Solvent (CSS) method. b) Powder X-ray diffraction patterns of raw PSZ, raw 4AMB and theoretical PSZ-4AMB cocystal from the Cambridge Structural Database (CSD)[17] and DoE samples processed by the CSS method. Experimental conditions as described in Table 2 (DoE Points 9-16). Red dotted lines, highlighting characteristic cocystal peaks, are included at 5.5° , 10.5° , 13° and 22.8° 2 Theta.

In this DoE, only one sample (DoE point 9) produced high purity PSZ with a minor amount of cocystal peaks detected. This sample was processed at the conditions that will dissolve the least amount of starting materials (low temperature and pressure) and this is likely to be the reason for few PSZ-4AMB cocystal peaks. Despite peaks at 19° , 22° and 25° 2 Theta corresponding to the PSZ-4AMB cocystal pattern, the cocystal is present in small amounts for this sample due to the low amount of peaks detected, relative to peaks corresponding to PSZ and 4AMB. The cause of this outcome likely involves an insufficient solubility of PSZ and 4AMB in the scCO_2 media at the processing conditions used in the DoE point 9, which involved using a lower pressure (100 bar) and temperature (35°C) and thereby a lower CO_2 density. Additionally, the low stirring rate (100 RPM)

may have negatively impacted negatively the cocrystallization of PSZ with 4AMB. This is supported by Padrela et al. who reported that processing several cocrystals by the CSS method without stirring resulted in impure cocrystallization, while a stirring rate of 300 RPM resulted in the complete cocrystallization of three different APIs (e.g. carbamazepine, indomethacin, theophylline) out of six.[44] The other DoE points (DoE points 10-16) at which samples were produced showed a significant number of peaks corresponding to the PSZ-4AMB cocrystal alongside several PSZ and 4AMB peaks indicating impure PSZ-4AMB samples were generated by the CSS method. Additionally, peaks at 13.9° and 15.4° 2θ for DoE points 9, 10, 13 and 15 appear to correspond to the raw 4AMB PXRD pattern indicating that incomplete cocrystallization may be the cause of the reduced cocrystal purity at these DoE points. As proposed above for DoE point 9, this is more than likely caused by the inadequate solubility of the starting materials in $scCO_2$. [46] The purity of this cocrystal may be improved by increasing reaction time [44] or by adding a cosolvent to the reaction mixture, as reported elsewhere. [45] As a result, an additional study using the CSS method where the hold time of two samples (DoE points 9 and 10) was increased to 8 hours (instead of 1 hour). The results of this study can be found in the supplementary material, Fig. SM6 but showed no significant differences in PXRD data compared to those presented in Fig. 6b.

Figure 7 depicts SEM micrographs and PSD analysis of DoE points (9-16) of PSZ-4AMB samples produced by the CSS method

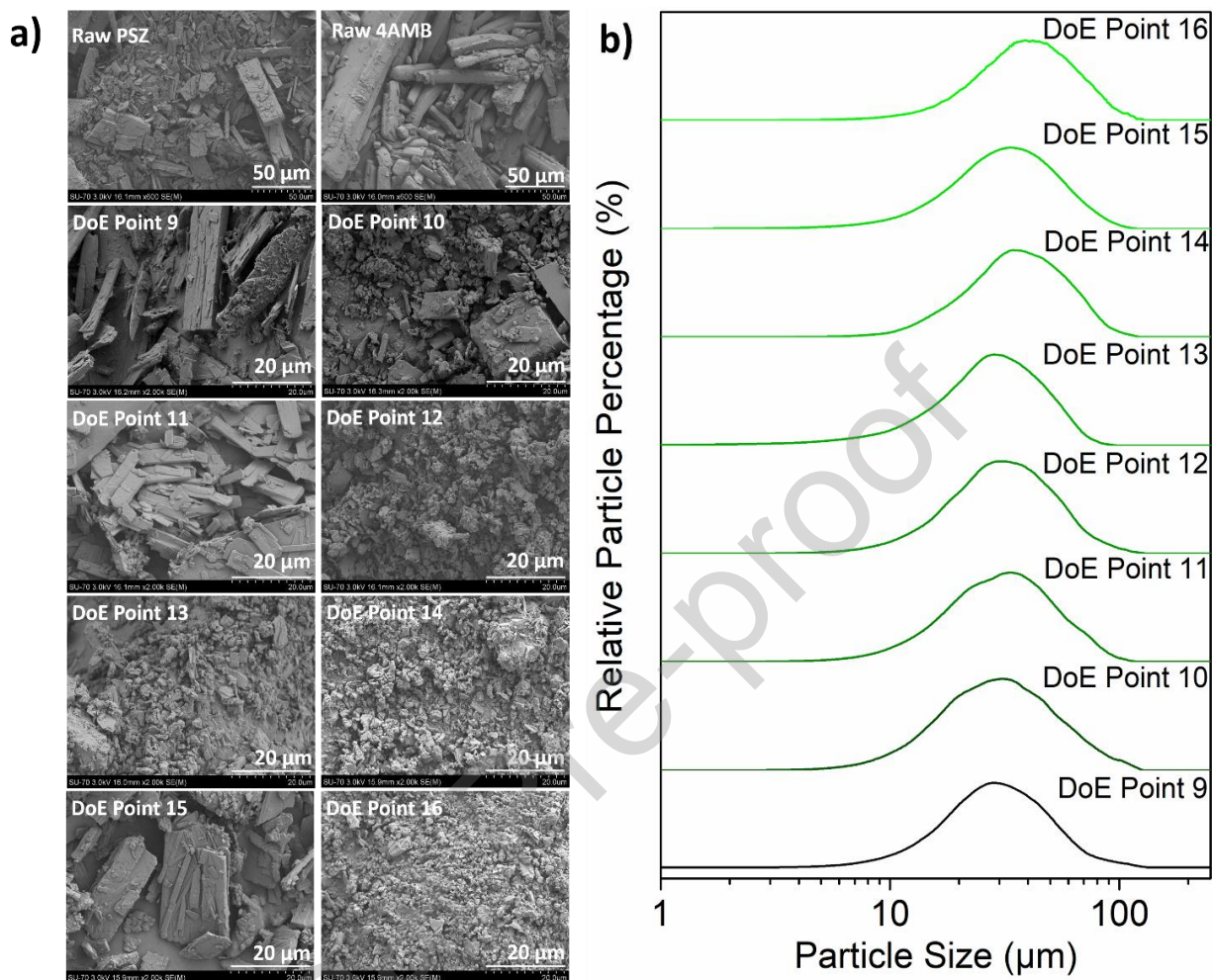


Figure 7. a) Scanning electron microscopy micrographs of raw PSZ, 4AMB and PSZ-4AMB samples (DoE points 9-16) and b) particle size distribution (PSD) of PSZ-4AMB samples (DoE Points 9-16) produced by the CocrySTALLization with Supercritical Solvent (CSS) method.

The sample which demonstrated a great similarity to the sample from DoE point 9 (mostly composed of PSZ as analysed by PXRD in Fig. 6b) shows long plate-shaped particles. The SEM micrographs for the CSS samples from DoE points 10, 11 and 15 shown in Fig. 7a present the same plate-like particle shapes but slightly smaller, more similar to the GAS samples (DoE points 1-8) observed in Fig. 4a. The CSS samples produced for DoE points 12, 13, 14 and 16 appear to demonstrate a smaller particle size than compared to the other points. This may be explained by the

high stirring rate (1000 RPM) experienced by DoE points 13, 14 and 16 which may have caused increased particle breakages. In the CSS method, raw forms of the API and coformer with larger particle sizes than each sample (DoE points 9-16) produced, are placed in their solid state in the vessel and are more susceptible to particle breakages due to only a small proportion of the API and coformer being dissolved in sCO₂ during processing. In Fig. 7b, the PSD of each CSS sample is presented. The average particle diameter for the CSS method ranges from 32 – 42 µm, which is marginally smaller than those produced by the GAS method. Although the SEM micrographs in Fig. 7a appear to show greater variation in particle sizes, all CSS samples (DoE points 9-16) demonstrate minor deviation from the median particle size value (36 µm) and, therefore, it is not possible to suggest that any processing condition influenced the PSD, based on this information. Similar to Fig. 4, the SEM micrographs in Fig. 7a are intended to provide information about the crystal habit, while the PSD analysis in Fig. 7b should be used to determine the particle size of the samples. The two operating parameters (high temperature and high pressure) which produced the smallest particle sizes using the GAS method (Fig. 4b) do not produce the same below average mean particle diameter when employing the CSS method. However, as the PSD variation using this method is relatively small, it is difficult to determine if any operating parameter had a significant impact towards the final particle size.

Figure 8 presents the DSC data for CSS samples for DoE points 9-16.

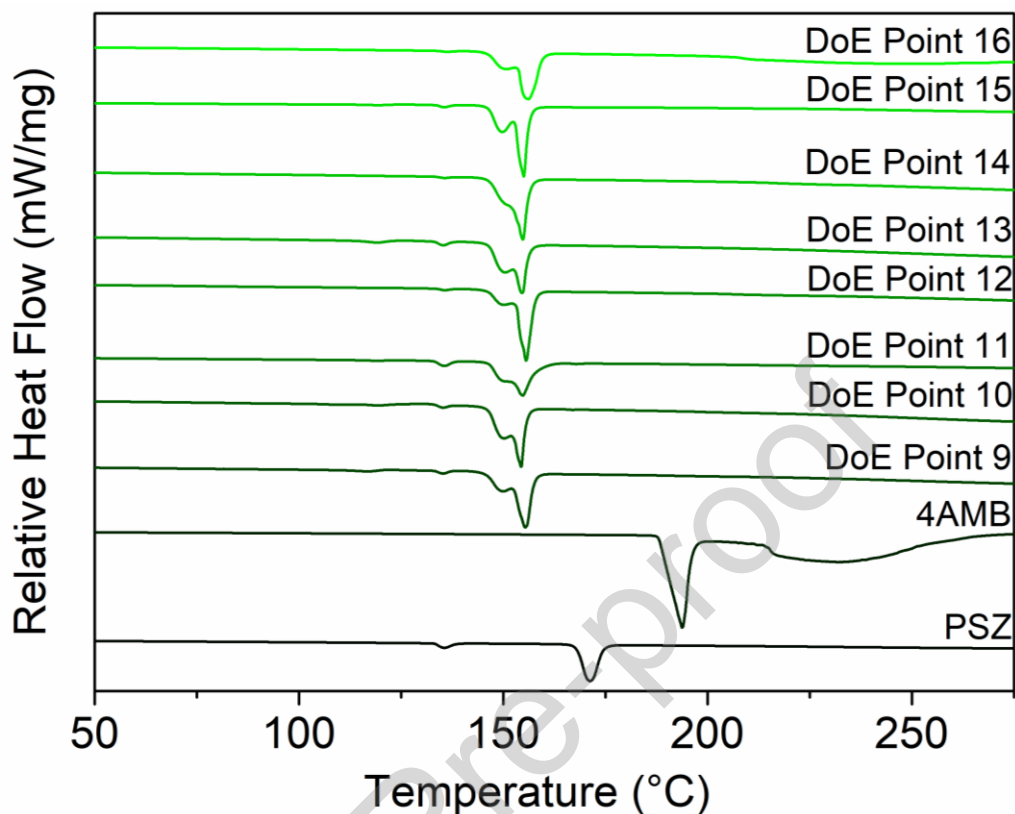


Figure 8. Differential scanning calorimetry (DSC) thermograms of raw PSZ, raw 4AMB and samples for DoE points 9-16, produced by the CSS method.

In each of these samples, a melting point at 154 °C accompanied by a shoulder peak at 148 °C is observed, the former corresponding to the PSZ-4AMB cocrystal. Kuminek et al. reported that the DSC thermograms of the pure PSZ-4AMB cocrystal show a single sharp melting peak at 154 °C with no other melting events.[17] The shoulder peak shown in Fig. 8 may represent impurities corresponding to the starting materials (PSZ or 4AMB) which is supported by the presence of PSZ PXRD peaks in Fig. 6b. The sample corresponding to DoE point 9 which produced a majority of characteristic PXRD peaks at 8, 10 and 18° 2 Theta corresponding to PSZ, unexpectedly showed a melting event at 154 °C representative of the cocrystal thermal behaviour. A melting event at 134 °C, corresponding to the PSZ nematic-like phase transition, can be observed at for all DoE points indicating the presence of PSZ, verified by PXRD results in Fig. 6b. Additionally, all samples

possess a shoulder peak at 148 °C indicating the presence of single components (API/coformer) or a physical mixture, also confirmed by the detection of PSZ peaks in the PXRD data in Fig. 6b. Overall, each sample produced by the CSS method demonstrated the presence of impurities, a result supported by the PXRD data from Fig. 6b.

3.3 Comparison of PSZ-4AMB material produced by GAS and CSS methods

Samples produced by GAS and CSS methods were compared to one another to highlight the primary differences between particles of PSZ-4AMB produced by each method. Beginning with the PXRD and purity of the samples, it was observed that the GAS method produced PSZ-4AMB cocrystal samples of higher purity than those prepared by the CSS method. Samples produced by the CSS method showed a significant presence of characteristic peaks of PSZ in the PXRD patterns when compared to those produced by the GAS method, indicating that the reaction between PSZ and 4AMB had not been fully completed. This is supported by the reported use of cosolvent to obtain higher purity samples when using the CSS method.[45] Reaction time was investigated as a possible reason for these low-purity samples but was determined to not be an influencing factor. This result highlights the greater likelihood of success for the GAS method and this is evidenced by its popularity, compared to the CSS technique which requires additional process optimization and is dependent on the solubility of starting material (API and coformer) in scCO₂. Two samples from each method (DoE points 4 and 9) demonstrated a high content of PSZ, indicating that a partial conversion (DoE point 4) or no conversion (DoE point 9) had occurred. The only processing condition that both of these DoE points shared was a low stirring rate (100 RPM). We propose that at these conditions, there is insufficient mixing between scCO₂, organic solvent, API and coformer (GAS method) or between API and coformer (CSS method) to facilitate cocrystallization. This

claim is supported by other researchers who have shown that a lower agitation requires a longer time to reach equilibria and may lead to incomplete reactions or impure cocrystals. [44, 50]

The SEM micrographs from samples produced by both GAS and CSS methods appeared to be quite similar in habit. These habits matched that of raw PSZ, introducing some limitations involving identification through this characterization technique. The PSD of both samples were recorded and revealed that both methods (GAS and CSS) produced mean particle sizes lower than 45 μm . The range of these particle sizes appear to correspond to those previously reported for another API (e.g. carbamazepine) using the GAS method.[22] However, the particles produced in this work by the CSS method appear to be smaller than those reported in literature which may be dependent on the cocrystal system or processing variables employed.[22] Padrela et al. and Cuadra et al. reported particle sizes ranging from 50 to 600 μm during the cocrystallization of indomethacin-saccharin and 5-fluorouracil cocrystals, respectively, using the CSS method.[42] When comparing both methods, this analysis showed that the median particle size of samples produced by the CSS (35.5 μm) method were marginally smaller than those produced by the GAS method (35.9 μm). However, the difference in the median particle size for each method was less than 1 μm and therefore, does not appear to present significant differences that can be achieved by either method.

The DSC data overall showed a melting point at 154 $^{\circ}\text{C}$, corresponding to the PSZ-4AMB cocrystal, at all but one DoE points (DoE point 4) for both methods, including the sample (DoE point 9) which presented a low presence of PSZ-4AMB from the PXRD data in Fig. 6b. However, due to the absence of a melting point at 188 $^{\circ}\text{C}$, corresponding to 4AMB, cocrystallization caused during DSC characterization may have occurred. This method was first reported by Lu et al. as an approach for

the rapid screening of cocrystals and may be the reason for the absence of the 4AMB melting point.[51] However, upon further investigation through DSC analysis of a physical mixture of PSZ and 4AMB, the absence of an exothermic peak suggests that it is unlikely that cocrystallization occurred during this characterization step. The presence of a shoulder peak at 148 °C was more apparent and pronounced for samples produced by the CSS method supporting the PXRD data that suggested these samples were lower in purity than those produced by the GAS method. Two samples which showed the sharpest DSC melting point at 154 °C, indicating a higher-purity cocrystal, were DoE points 5 and 6, produced by the GAS method. This result is supported by the PXRD data which shows the lowest presence of peaks corresponding to PSZ from any sample. Overall, these high purity cocrystal samples emphasize that the GAS method is the more favorable method to generate the PSZ-4AMB with further optimization required to generate similar purity cocrystals by the CSS method.

4.0 Conclusions

Cocrystallization of the antifungal drug Posaconazole with 4-Aminobenzoic acid has been achieved for the first time using two unique scCO₂ methods, namely Gas Antisolvent (GAS) and Cocrystallization with Supercritical Solvent (CSS) methods, in which scCO₂ acts as an antisolvent and solvent, respectively. The PSZ-4AMB cocrystal produced from GAS and CSS methods exhibit the same crystal structure and melting point as those recently obtained by different methodologies.[17]

Starting with the GAS method, a DoE approach was applied to investigate the impact of critical processing parameters (pressure, temperature and stirring rate) on PSZ-4AMB formation, size and

habit. Out of 8 different processing points, 7 of these produced the PSZ-4AMB cocrystal with minor impurities belonging to single entity PSZ, which are also observed in the first reports of this cocrystal. Size and habit did not appear to be significantly influenced by any of the three critical processing parameters and a narrow PSD was obtained for the majority of DoE points. The only sample which did not produce PSZ-4AMB was completed at high temperature, pressure and low stirring rate (65 °C, 20.0 MPa and 100 RPM, respectively) which may favor single entity PSZ in a quaternary phase diagram.

The CSS method demonstrated additional challenges when attempting to generate high purity cocrystal samples. Similar to the GAS method, 7 out of a possible 8 DoE points demonstrated a significant number of PXRD peaks corresponding to the theoretical pattern of PSZ-4AMB, however these samples also contained impurities corresponding to PSZ. The sample (DoE point 9) which demonstrated a significant proportion corresponding to PSZ was generated using low temperature, pressure and stirring rate (35 °C, 10.0 MPa and 100 RPM, respectively). The reduced solubility of API and coformer at these moderate conditions may have reduced the solubility of both starting materials in scCO₂ causing inadequate interaction between PSZ and 4AMB to produce the cocrystal material. The remaining samples demonstrated a higher number of peaks matching the characteristic peaks of the PSZ-4AMB cocrystal theoretical pattern. However, these samples also presented impurities matching PSZ and would require further optimization to achieve a complete cocrystallization of PSZ-4AMB. An additional preliminary study investigating an increased reaction time (8 hours instead of 1) on some DoE points did not demonstrate any significant improvement towards cocrystal purity.

Comparing GAS and CSS methods, both approaches generate particles with a mean diameter of less than 45 µm, with the CSS method producing marginally smaller samples. Both methods produce a

narrow PSD for the majority of DoE points. Single entity PSZ and the PSZ-4AMB cocrystal demonstrate similar plate-like particle shapes using GAS and CSS methodologies.

Overall, the GAS method has been shown to be a viable method to produce high purity samples of the cocrystal PSZ-4AMB. The CSS method was also shown to produce PSZ-4AMB samples without the requirement for organic solvent, however these samples were lower in purity than those produced by GAS. An interesting point worth further exploration would be to investigate the use of a cosolvent towards optimization of the CSS method. The cosolvent may facilitate increased intermolecular interactions between API and cofomer and lead to a high purity cocrystal system.

Declaration of Competing Interest

None.

Acknowledgements

This work was undertaken as part of the Synthesis and Solid State Pharmaceutical Centre supported by the Science Foundation Ireland (SFI) and is co-funded under the European Regional Development Fund (Grants SFI SSPC2 12/RC/2275 and 15/US-C2C/I3133). The work was also supported by Enterprise Ireland (Grant CF-2017-0754). We would also like to thank Dr. Suresh Sanda (University of Limerick, Ireland) for assisting with PSD analysis.

Appendix A. Supplementary Data

Supplementary material provided.

References

- [1] N. Schultheiss, A. Newman, *Pharmaceutical Cocrystals and Their Physicochemical Properties*, *Crystal Growth & Design*, 9 (2009) 2950-2967.
- [2] D.D. Gadade, S.S. Pekamwar, *Pharmaceutical Cocrystals: Regulatory and Strategic Aspects*, *Design and Development*, *Adv Pharm Bull*, 6 (2016) 479-494.
- [3] F.a.D.A.-U.S.D.o. Health, *Regulatory Classification of Pharmaceutical Co-Crystals Guidance for Industry*, (2018).
- [4] R. Shaikh, R. Singh, G.M. Walker, D.M. Croker, *Pharmaceutical cocrystal drug products: an outlook on product development*, *Trends in pharmacological sciences*, 39 (2018) 1033-1048.
- [5] Ö. Almarsson, M.J. Zaworotko, *Crystal engineering of the composition of pharmaceutical phases. Do pharmaceutical co-crystals represent a new path to improved medicines?*, *Chemical communications*, (2004) 1889-1896.
- [6] S. Aitipamula, R. Banerjee, A.K. Bansal, K. Biradha, M.L. Cheney, A.R. Choudhury, G.R. Desiraju, A.G. Dikundwar, R. Dubey, N. Duggirala, *Polymorphs, salts, and cocrystals: what's in a name?*, *Crystal growth & design*, 12 (2012) 2147-2152.
- [7] A. Kumar, S. Kumar, A. Nanda, *A review about regulatory status and recent patents of pharmaceutical co-crystals*, *Advanced pharmaceutical bulletin*, 8 (2018) 355.
- [8] D. Braga, F. Grepioni, L. Maini, S. Prosperi, R. Gobetto, M.R. Chierotti, *From unexpected reactions to a new family of ionic co-crystals: the case of barbituric acid with alkali bromides and caesium iodide*, *Chemical Communications*, 46 (2010) 7715-7717.
- [9] D. Braga, F. Grepioni, G.I. Lampronti, L. Maini, A. Turrina, *Ionic Co-crystals of Organic Molecules with Metal Halides: A New Prospect in the Solid Formulation of Active Pharmaceutical Ingredients*, *Crystal Growth & Design*, 11 (2011) 5621-5627.
- [10] D. Braga, L. Maini, F. Grepioni, *Mechanochemical preparation of co-crystals*, *Chemical Society Reviews*, 42 (2013) 7638-7648.
- [11] N. Shan, M.J. Zaworotko, *The role of cocrystals in pharmaceutical science*, *Drug Discovery Today*, 13 (2008) 440-446.
- [12] N.K. Duggirala, M.L. Perry, Ö. Almarsson, M.J. Zaworotko, *Pharmaceutical cocrystals: along the path to improved medicines*, *Chemical Communications*, 52 (2016) 640-655.
- [13] D.P. Elder, R. Holm, H.L.d. Diego, *Use of pharmaceutical salts and cocrystals to address the issue of poor solubility*, *International Journal of Pharmaceutics*, 453 (2013) 88-100.
- [14] O.N. Kavanagh, D.M. Croker, G.M. Walker, M.J. Zaworotko, *Pharmaceutical cocrystals: from serendipity to design to application*, *Drug Discovery Today*, 24 (2019) 796-804.
- [15] P. Tang, L. Wang, X. Ma, K. Xu, X. Xiong, X. Liao, H. Li, *Characterization and In Vitro Evaluation of the Complexes of Posaconazole with β - and 2,6-di-O-methyl- β -cyclodextrin*, *AAPS PharmSciTech*, 18 (2017) 104-114.
- [16] G.M. Keating, *Posaconazole*, *Drugs*, 65 (2005) 1553-1567.
- [17] G. Kuminek, K.L. Cavanagh, M.F.M. da Piedade, N. Rodríguez-Hornedo, *Posaconazole Cocrystal with Superior Solubility and Dissolution Behavior*, *Crystal Growth & Design*, 19 (2019) 6592-6602.
- [18] S.U. Din, H. Hughes, N.J. O'Reilly, H. Cathcart, T. O'Ceallaigh, E. Ndzie, P. McLoughlin, *Investigation into the Stability, Crystallization Kinetics, and Heating Rate Dependent Crystallization of Amorphous Posaconazole*, *Crystal Growth & Design*, (2020).
- [19] D.K. McQuiston, M.R. Mucalo, G.C. Saunders, *The structure of posaconazole and its solvates with methanol, and dioxane and water: Difluorophenyl as a hydrogen bond donor*, *Journal of Molecular Structure*, 1179 (2019) 477-486.

- [20] I.A. Cuadra, A. Cabañas, J.A.R. Cheda, C. Pando, Polymorphism in the co-crystallization of the anticonvulsant drug carbamazepine and saccharin using supercritical CO₂ as an anti-solvent, *The Journal of Supercritical Fluids*, 136 (2018) 60-69.
- [21] B. Long, K.M. Ryan, L. Padrela, From batch to continuous—New opportunities for supercritical CO₂ technology in pharmaceutical manufacturing, *European Journal of Pharmaceutical Sciences*, (2019) 104971.
- [22] L. Padrela, M.A. Rodrigues, A. Duarte, A.M. Dias, M.E. Braga, H.C. de Sousa, Supercritical carbon dioxide-based technologies for the production of drug nanoparticles/nanocrystals—a comprehensive review, *Advanced drug delivery reviews*, 131 (2018) 22-78.
- [23] C. Harscoat-Schiavo, C. Neurohr, S. Lecomte, M. Marchivie, P. Subra-Paternault, Influence of isomerism on recrystallization and cocrystallization induced by CO₂ as an antisolvent, *CrystEngComm*, 17 (2015) 5410-5421.
- [24] N. Wichianphong, M. Charoenchaitrakool, Application of Box–Behnken design for processing of mefenamic acid–paracetamol cocrystals using gas anti-solvent (GAS) process, *Journal of CO₂ Utilization*, 26 (2018) 212-220.
- [25] N. Wichianphong, M. Charoenchaitrakool, Statistical optimization for production of mefenamic acid–nicotinamide cocrystals using gas anti-solvent (GAS) process, *Journal of Industrial and Engineering Chemistry*, 62 (2018) 375-382.
- [26] C. Pando, A. Cabanas, I.A. Cuadra, Preparation of pharmaceutical co-crystals through sustainable processes using supercritical carbon dioxide: a review, *RSC advances*, 6 (2016) 71134-71150.
- [27] L. MacEachern, A. Kermanshahi-pour, M. Mirmehrabi, Supercritical Carbon Dioxide for Pharmaceutical Co-Crystal Production, *Crystal Growth & Design*, (2020).
- [28] A.S. Pessoa, G.P.S. Aguiar, J.V. Oliveira, A.J. Bortoluzzi, A. Paulino, M. Lanza, Precipitation of resveratrol-isoniazid and resveratrol-nicotinamide cocrystals by gas antisolvent, *The Journal of Supercritical Fluids*, 145 (2019) 93-102.
- [29] G. Kotbantao, M. Charoenchaitrakool, Processing of ketoconazole–4-aminobenzoic acid cocrystals using dense CO₂ as an antisolvent, *Journal of CO₂ Utilization*, 17 (2017) 213-219.
- [30] M.M. Ribas, G.S. Sakata, A.E. Santos, C. Dal Magro, G.P.S. Aguiar, M. Lanza, J.V. Oliveira, Curcumin cocrystals using supercritical fluid technology, *The Journal of Supercritical Fluids*, 152 (2019) 104564.
- [31] C. Neurohr, A.-L. Revelli, P. Billot, M. Marchivie, S. Lecomte, S. Laugier, S. Massip, P. Subra-Paternault, Naproxen–nicotinamide cocrystals produced by CO₂ antisolvent, *The Journal of Supercritical Fluids*, 83 (2013) 78-85.
- [32] A. Shikhar, M.M. Bommana, S.S. Gupta, E. Squillante, Formulation development of Carbamazepine–Nicotinamide co-crystals complexed with γ -cyclodextrin using supercritical fluid process, *The Journal of Supercritical Fluids*, 55 (2011) 1070-1078.
- [33] M.M. Ribas, G.P.S. Aguiar, L.G. Muller, A.M. Siebel, M. Lanza, J.V. Oliveira, Curcumin-nicotinamide cocrystallization with supercritical solvent (CSS): Synthesis, characterization and in vivo antinociceptive and anti-inflammatory activities, *Industrial Crops and Products*, 139 (2019) 111537.
- [34] L. Padrela, B. Castro-Dominguez, A. Ziaee, B. Long, K.M. Ryan, G. Walker, E. O'Reilly, Co-crystal polymorphic control by nanodroplet and electrical confinement, *CrystEngComm*, 21 (2019) 2845-2848.
- [35] P. Gallagher, M. Coffey, V. Krukonis, N. Klasutis, Gas antisolvent recrystallization: new process to recrystallize compounds insoluble in supercritical fluids, in, *ACS Publications*, 1989.

- [36] V.J. Krukonis, P. Gallagher, M. Coffey, Gas anti-solvent recrystallization process, in, Google Patents, 1994.
- [37] E. Said-Galiyev, I. Pototskaya, Y.S. Vygodskii, Supercritical carbon dioxide and polymers, *Polymer Science, Series C: Reviews*, 46 (2004) 1-13.
- [38] B. Long, K.M. Ryan, L. Padrela, Investigating Process Variables and Additive Selection To Optimize Polymorphic Control of Carbamazepine in a CO₂ Antisolvent Crystallization Process, *Organic Process Research & Development*, (2020).
- [39] H.S. Byun, B.M. Hasch, M.A. McHugh, Phase behavior and modeling of the systems CO₂-acetonitrile and CO₂-acrylic acid, *Fluid Phase Equilibria*, 115 (1996) 179-192.
- [40] N. Esfandiari, S.M. Ghoreishi, Ampicillin Nanoparticles Production via Supercritical CO₂ Gas Antisolvent Process, *AAPS PharmSciTech*, 16 (2015) 1263-1269.
- [41] I.A. Cuadra, F. Zahran, D. Martín, A. Cabañas, C. Pando, Preparation of 5-fluorouracil microparticles and 5-fluorouracil/poly(l-lactide) composites by a supercritical CO₂ antisolvent process, *The Journal of Supercritical Fluids*, 143 (2019) 64-71.
- [42] L. Padrela, M.A. Rodrigues, S.P. Velaga, H.A. Matos, E.G. de Azevedo, Formation of indomethacin–saccharin cocrystals using supercritical fluid technology, *European Journal of Pharmaceutical Sciences*, 38 (2009) 9-17.
- [43] A. Tavana, A.D. Randolph, Manipulating solids CSD in a supercritical fluid crystallizer: CO₂-benzoic acid, *AIChE Journal*, 35 (1989) 1625-1630.
- [44] L. Padrela, M.A. Rodrigues, J. Tiago, S.P. Velaga, H.A. Matos, E.G. de Azevedo, Insight into the Mechanisms of Cocrystallization of Pharmaceuticals in Supercritical Solvents, *Crystal Growth & Design*, 15 (2015) 3175-3181.
- [45] I.A. Cuadra, A. Cabañas, J.A.R. Cheda, M. Türk, C. Pando, Cocrystallization of the anticancer drug 5-fluorouracil and cofomers urea, thiourea or pyrazinamide using supercritical CO₂ as an antisolvent (SAS) and as a solvent (CSS), *The Journal of Supercritical Fluids*, (2020) 104813.
- [46] G. Tian, J. Jin, Z. Zhang, J. Guo, Solubility of mixed solids in supercritical carbon dioxide, *Fluid Phase Equilibria*, 251 (2007) 47-51.
- [47] F.F.a.D. Administration), *CLINICAL PHARMACOLOGY AND*

BIOPHARMACEUTICS REVIEW APPLICATION NUMBER:

205053Orig1s000, in, 2013.

- [48] M. Svärd, F.L. Nordström, E.-M. Hoffmann, B. Aziz, Å.C. Rasmuson, Thermodynamics and nucleation of the enantiotropic compound p-aminobenzoic acid, *CrystEngComm*, 15 (2013) 5020-5031.
- [49] C.J. Chang, The solubility of carbon dioxide in organic solvents at elevated pressures, *Fluid Phase Equilibria*, 74 (1992) 235-242.
- [50] M.J. Cocero, S. Ferrero, Crystallization of β -carotene by a GAS process in batch Effect of operating conditions, *The Journal of Supercritical Fluids*, 22 (2002) 237-245.
- [51] E. Lu, N. Rodríguez-Hornedo, R. Suryanarayanan, A rapid thermal method for cocrystal screening, *CrystEngComm*, 10 (2008) 665-668.

Declaration of interests

The authors declare that they have no known competing financial interests or personal relationships that could have appeared to influence the work reported in this paper.

The authors declare the following financial interests/personal relationships which may be considered as potential competing interests:

Journal Pre-proof

Highlights

- Cocrystals of antifungal drug Posaconazole (PSZ) were prepared with 4-Aminobenzoic Acid (4AMB).
- The PSZ-4AMB cocrystal was prepared by Gas Antisolvent (GAS) and Cocrystallisation with a Supercritical Solvent (CSS) methods.
- The GAS method led to a higher purity cocrystal compared to the CSS method.
- The GAS and CSS methods produced particle sizes (D_{50}) ranging from 20 - 43 μm and 32 - 42 μm , respectively.

Journal Pre-proof